



SIMULTANEOUS SIMULATION FOR KOBE:WHAT WE HAVE LEARNED AT ESG98

Hiroshi KAWASEA¹ And Tomotaka IWATA²

SUMMARY

We conducted the open simultaneous simulation for Hyogo-ken Nanbu (Kobe) earthquake as a special effort for the second International Symposium on the Effects of Surface Geology (ESG) on Strong Motion held in Yokohama in 1998. In this simulation voluntary participants were asked to simulate strong motions at predefined locations in Kobe and Osaka. One half of the sites have observed records during the mainshock as well as aftershocks, which are distributed before the simulation. We received finally 19 group of participants, 16 of which succeeded to send us their digital synthetics in a timely manner. We summarize here these submitted results in terms of their methods and models, points of their main concern, peak ground velocity values, and velocity waveforms in comparison to the observed data. These simulations cover the current state-of-the-art of the simulation methodology for ESG. The most important conclusion is that the level of variation among the simulated results is much higher for the blind sites at which no observed records were available than for the open sites at which we distribute the observed records. This means that the more we observe, the better we predict.

INTRODUCTION

We summarize here the results submitted by the participants of the Simultaneous Simulation (S.S.) experiment for the Hyogo-ken Nanbu (Kobe) earthquake, which was conducted by the local organizing committee of the second International Symposium on the Effects of Surface Geology on Strong Motions (ESG98) held in Yokohama in December 1 to 3, 1998. The details of the simulation rules and distributed data are mentioned by the accompanied paper [Iwata et al., 1999]. We defined two simulation lines, one in Kobe and the other in Osaka, along which participants are requested to generate their own synthetics by their preferred methods and models. We first briefly mention their methods, models, and points. Then we show peak ground velocities (PGVs) and velocity waveforms in comparison with the observed ones. The purpose of the S.S. is not the competition, and therefore we do not put much emphasis on the matching of the individual simulation with the observed. Rather, we focus our attention mainly the inter-site and inter-simulation variability. If only one method tends to overestimate the ground motions for most of the sites or if at only one site most methods tend to overestimate, then we should search the reason. From the comparison we can delineate what are the controlling parameters on the near-field strong motion in Kobe or moderately-distant basin response in Osaka.

A BRIEF SUMMARY OF THE METHODS

As a final number we received simulations from 19 research groups in total. Among these 19 parties, 16 has succeeded to send us their digital synthetics in a timely manner. This means that, to our regret, the results of the three parties are not covered here. We divide all the 19 results into two groups, one of which (consists of 6 parties) focus their attention to the three-dimensional modeling of the ground, and the other of which (consists of 13 parties) uses variety of methods such as the empirical or statistical Green's function methods, hybrid methods,

¹ Graduate School of Human Environment Studies, Kyushu University, Fukuoka, Japan. kawase@seis.arch.kyushu-u.ac.jp

² Disaster Prevention Research Institute, Kyoto University, Uji, Japan. iwata@egmpri01.dpri.kyoto-u.ac.jp

and 1-D or 2-D nonlinear response calculation. A couple of participants do not cover all the stations at which we asked to calculate synthetics, that is, six for Kobe and six for Osaka, but anybody who submitted their results for more than one station are processed and presented here. Note that this S.S. is not a competition so that we did not put high priority on treating everybody as fair as possible. Rather, we tried to encourage participants to submit their simulations no matter how small percentage of the specified obligations they actually fulfilled. During the symposium ESG98 a few participants complained our treatment on this regard, but we believe that our policy resulted in many varieties of participants and simulated results shown here.

Among 16 parties, 15 of them simulate ground motions along the Kobe line and 5 simulate those along the Osaka line. This is quite well understood since the level of shaking is stronger in the Kobe line and so people are more concerned. Technically speaking responses in Kobe are easier to calculate by the domain-type method such as 3-D finite difference since we need less analyzing space. This does not mean at all that the simulation along the Kobe line is easier than the other. Since locations of the sites in the Kobe line are very close to the seismogenic fault in Kobe, we must represent both the source and the ground response quantitatively. On the other hand, along the Osaka line, which is about 50 km away from the fault, characteristics of strong motions there are mainly controlled by the basin response and so its representation should be more important.

Tables 1 and 2 summarize paper titles, methods and models used, sites and types of waveforms (acc. or vel.) simulated, and main foci of simulation for all the 16 parties. Note that ID number of each party starts from SS04 and that we do not have digital data for SS10 to SS12. Detailed description of the simulations is found in the corresponding paper collected in the third volume of the ESG98 proceedings [Irikura et al. 1999]. Among six simulation using 3-D basin models (SS04 to SS09), only one (SS04) is for Osaka and the remaining five are for Kobe. We can directly compare these five simulations. Among ten simulations not based on the 3-D modeling (SS13 to SS22), four of them incorporate the nonlinear site response due to liquefaction and so comparison among them will be quite interesting. Note that not all the parties provide three component synthetics at each site.

PEAK VELOCITY AND ACCELERATION

Next we summarize peak ground velocities (PGVs) and peak ground accelerations (PGAs) of 16 simulated results. Accelerograms are used only if participants provided them, while velocity synthetics are calculated if only accelerations are provided. We must note that several simulations, including most of the simulations with 3-D basin models, do not cover sufficient high frequency range to obtain quantified acceleration, but here we plot their nominal values no matter how low or high their frequency limits are. Fig.1 shows PGVs of all the submitted synthetics at KBU, a rock (exactly speaking, very close to rock) site in the Kobe line. Stars denote the observed values for different component and thick horizontal lines with shaded bands denote the average PGVs and average plus/minus one standard deviation. As mentioned above, parties from SS05 to SS09 used 3-D basin models while parties from SS13 to SS18 used their own variation of stochastic or empirical Green's function methods. Note that because of the stochastic nature of the method PGVs and PGAs of SS13 should be considered as one sample realization among possible cases.

On the average simulated PGVs shown in Fig.1 are very close to the observed (with one exception, EW component of SS14) and the standard deviations of all the simulated results are much smaller than we expected before the S.S., especially in the NS component. The reason why most of the simulations succeeded to reproduce PGV values at KBU may be a) source processes assumed are probably well calibrated by the KBU record and b) site effects at KBU must be minimal since it lies inside a tunnel the bottom of which is very close to the surface of the Rokko granite [Iwata et al., 1999]. As is the case of SS18, participants can also tune-up their results by using the observed record as a control motion. This can only be done for "postdiction" like the S.S. here, in which the observed data are provided for the target earthquake as well as its aftershocks.

Fig.2 shows PGVs at RKI, a southmost reclaimed-land site in the Kobe line, in the same manner as in Fig.1. In this case inter-simulation variation is much larger than that at KBU as an absolute velocity value. But if we look at the coefficients of variation (C.O.V. = standard deviation / the average) for two horizontal components, they are similar to KBU and are about 30 to 40 percent as shown in Table 3. The averaged values are close to the observed for two horizontal components while it is about two times larger than the observed for the vertical component. We found that simulations with 2-D or 3-D basin structure tend to overestimate the observed PGV in the UD component at RKI. As seen in Table 3 C.O.V. tends to be higher for vertical component.

If we look at PGVs for blind prediction sites in the Kobe line, namely, KB1, KB2, KB3, and KB4, we can see that averaged PGVs for NS component are increasing from KBU (44 cm/s) to KB3 (102 cm/s) and then

decreasing to RKI (84 cm/s). This corresponds to the damage distribution found in Nada-ku and Higashinada-ku in Kobe and should be caused by the edge effect [Kawase 1996, Kawase et al. 1999] if the method used is incorporated with 2-D or 3-D basin structures. The simulations not incorporated with basin structures, namely, SS13, SS14, SS21, and SS22 do not show such clear spatial deviation along the Kobe line, although some inter-station variation exists because of their different sedimentary layers used in the analyses. Inter-simulation variations at these four blind sites are apparently larger than open (observed) sites, especially among parties from SS13 to SS22. Please refer to the averaged C.O.V. in Table 3 for open and blind sites including the Osaka line.

As for the PGAs again we omit figures here, but we found that even for accelerations agreement with the observed PGAs at KBU and RKI is very good on the average and the deviation from the average is relatively small. As is the case for PGVs variations for the blind sites are much larger than the open (observed) sites.

As for the Osaka line, we show here in Fig.3 PGVs at four sites, namely, OS5, FKS, OSA, and YAE aligned from west to east. We take the EW component as a representative one here. Among six sites in the Osaka line at most only five results are present and at least only three results are. Therefore, statistically valid judgment is difficult to derive from the submitted results. However, among these five simulations we can see the same degree of matching to the observed PGVs and the same degree of inter-simulation variation in the Kobe line. We found that with high probability the observed PGVs are very close to the PGVs averaged for SS4 and SS13. If this is the case for OS5, then the averaged PGV in the EW component shown here, 35 cm/s, may be too high due to one outlier, SS18 whose prediction is 60 cm/s. On the other hand, the averaged PGV for the vertical component at OS5, 20 cm/s, may be too high because of one outlier, SS04 whose prediction is 41 cm/s. SS04 tends to overestimate the vertical component as the site moves from east to west. We speculate that this may be caused by the relatively stiff shallow basin structure in the simulation, which results in a different H/V mode shape for Rayleigh wave. The similar phenomenon can be seen in the Kobe line, although propagation distance is rather short in Kobe.

COMPARISON OF VELOCITY WAVEFORMS

Next we compare velocity waveforms of the submitted synthetics with each other and with the observed ones. First the results of the Kobe line are shown. Fig.4 shows velocity waveforms observed (thick line) and simulated (thin line) for KBU, NS component. Synthetics are aligned to have a similar timing in the beginning of waveforms determined by sight, although sometimes our choice was not perfect. In such a case please find the best matching by your own judgement. As is the PGV values, velocity waveforms from SS05 to SS09 are remarkably similar to each other. If we look at them closely, we notice that each simulation has its own character. Among the other simulations from SS13 to SS18, SS15 and SS17 show very good fit to the observed waveforms. SS15 does so with good reason since its source model is specifically tuned for the records including KBU [Kamae and Irikura, 1998]. However, SS17 is based on the source process slightly modified from that of Sekiguchi et al. [1996] as shown in the proceedings, there must be another reason for this level of good fit. For EW component SS16 shows also good fit. As mentioned above, SS13 shown here is just one sample of the whole stochastic prediction and so we should not pay much attention to its individual phase matching.

As for the blind "postdiction" results at KB1 to KB4, which is omitted here, simulations from SS05 to SS09 give very similar waveform to each other, among which SS07 has the largest amplitude. This is probably caused by the softest and thickest surface layer assumed in this simulation, whose S-wave velocity is 333 m/s. Simulations from SS18 to SS22 generally give high velocity amplitude as has already mentioned in the previous section.

Fig.5 shows results at RKI with the observed waveform for NS component. In this case even among simulations from SS05 to SS09 differences become apparent after a couple of second from the onset of S-wave. Especially, SS06 and SS07 have stronger and higher-frequency arrivals of later phases than the observed. In general these simulations tend to generate waveforms with shorter predominant period which may be a direct consequence of nonlinearity not considered in these simulations. If we look at other simulations variations become more pronounced. We understand that those with 1-D soil models, namely SS13, SS14, and SS17 tend to underestimate the observed long duration, while those convolved with 2-D basin response, namely SS16, SS18, SS19, and SS20 have longer duration similar to the observed. As is the case with 3-D basin models, later phases in these simulations have shorter predominant periods than the observed. The long-period later phases can be seen in SS21 and SS22 where 1-D nonlinear soil response is considered. Note that SS21 has long-lasting and long-period later phases very similar to the observed. This matching is achieved primarily because they used an input motion deconvolved from the observed borehole record at Port Island, another site on the reclaimed land.

In Fig.6 we show EW component velocity waveforms along the Osaka line, at OS5, FKS, OSA, and YAE. When we compare these simulation with the observed we found that SS04 give quite similar results, which used a 3-D basin structure of Miyakoshi et al. [1997] distributed by the organizer [Iwata et al. 1999]. Especially at FKS and YAE overall matching is very good for the whole duration. At OSA, which is very close to the Uemachi fault, SS04 gives shorter-period, stronger later phases than the observed. In general SS04 tends to underestimate S-wave part and overestimate surface wave part, which probably comes from infinite Q values of the basin layers assumed by SS04. SS22 also reproduces overall characteristics of the observed waveforms, especially for sites in the eastern side (i.e., OSA and YAE), since they used the empirical Green's function method, together with nonlinear surface soil response. SS13 captures the main characteristics of the S-wave part of the observed records and SS18 tends to overestimate the S-wave part amplitude in the western-side stations such as OS5 and FKS.

COMPARISON OF RESPONSE SPECTRA

Finally we compare pseudo velocity response spectra of 5% damping. Here pseudo velocity response spectra are calculated from the absolute acceleration response spectra. Since our space is limited we only describe what we have obtained. At KBU the peak value of the observed response spectra reaches about 200 cm/sec at 1.2 second in the NS component, while at RKI peak values are the same level, 200 cm/s, for both components at about 2.5 second. It should note that for most of the 3-D simulations, SS05 to SS09, simulated response spectra at RKI have very prominent peaks, which is at slightly shorter period than the observed, around 2 seconds. In the response spectra SS16, SS17, SS21, and SS22 did a better job than the others. At RKI we found that majority of them tend to overestimate the peak level of the observed spectra. Since response spectra are the indicator of the peak value, they are basically proportional to the PGVs shown in Figs. 1 and 2.

For the Osaka line we also check the response spectra of all the observed waveforms and the simulated ones. Observed peak levels are about 50 cm/s to 100 cm/s with wider period range from 0.8 to 5 seconds. As is the waveform, SS04 and SS13 give quite similar results to the observed, however, they provide quite different results for the blind sites, namely, OS5 and OS6. SS18 tends to overestimate longer period component and SS20 gives common 1 second peak period for all the stations since they used FKS as a reference. SS22 gives high amplitude at the western sites but reasonable amplitude at the eastern sites, again as shown in the waveforms.

CONCLUSIONS

We show a part of the results of the Simultaneous Simulation for Kobe and summarize the most important points of the outcome. We found that the simulated results have small deviations in general and even smaller ones if the methods and models used are similar to each other. We also found that the deviations are smaller and the matching is better for sites with the observed data. This is encouraging because this means that our simulation is under the control of observed data. On the other hand this also sends us a warning signal; without the control of data we can get anything in the blind prediction. One thing we would like to emphasize here is that we should try to clarify the mechanisms of the waveform generation, propagation, and amplification as much as we can in order to fully understand the strong motion characteristics and to quantitatively predict strong motions from future destructive earthquakes. Just the final products presented are not sufficient to improve our knowledge and techniques for strong motion prediction. This is the beginning toward the goal of the ESG study.

ACKNOWLEDGEMENT

We express our sincere gratitude to all the participants of the Simultaneous Simulation for Kobe. Without their effort and cooperation we cannot reach this level of achievement. We also thank cooperative organizations that provided valuable observed records for this experiment. Ms. Sekiguchi at DPRI, Kyoto University helped us when we made figures using GMT.

REFERENCES

- Irikura, K., K. Kudo, H. Okada, and T. Sasatani (Eds.) [1999]. *Proc. of the 2nd International Symposium on the Effects of Surface Geology on Seismic Motion*, Vol.3, Balkema, Rotterdam.
- Iwata T., H. Kawase, H. Sekiguchi, S. Matsushima, A. Pitarka, and K. Irikura [1999]. "Standard basin structure model construction and strong ground motion simulation for Kobe", *Proc. of the 12th World Conf. Earth. Eng.*, CD-ROM, Oakland, New Zealand.
- Kamae, K. and K. Irikura, [1998]. "Source model of the 1995 Hyogoken Nanbu earthquake and simulation of near-source ground motion", *Bull. Seism. Soc. Am.*, 88, pp400-412.
- Kawase, H. [1996]. "The cause of the damage belt in Kobe: "The basin-edge effect", Constructive interference of the direct S-wave with the basin-induced diffracted/Rayleigh waves", *Seismological Research Letters*, 67, No.5, 25-34.
- Kawase, H., S. Matsushima, R.W. Graves, and P.G. Somerville [1999]. "Strong motion simulation of Hyogo-ken Nanbu (Kobe) earthquake considering both the heterogeneous rupture and the 3-D basin structure", *Proc. of the 12th World Conf. Earth. Eng.*, CD-ROM, Oakland, New Zealand.
- Miyakoshi, K, T. Kagawa, and T. Echigo [1997]. "On the modelization of deep sedimentary structure beneath the Osaka plain (2)", *Abstracts of 1997 Japan Earth and Planetary Sci. Joint Meeting*, B42-06 (in Japanese).
- Sekiguchi, H., K. Irikura, T. Iwata, Y. Kakehi, and M. Hoshiya, [1996]. "Minute locating of faulting beneath Kobe and the waveform inversion of the source process during the 1995 Hyogo-ken Nanbu, Japan, earthquake using strong ground motion records", *J. Phys. Earth*, 44, 473-487.

Table 1 List of submitted papers of S.S. for Kobe from SS04 to SS13 and their simulation outline

SS ##	Title of the paper (first author)	Method and Model	Simulated sites (values)	Main focus of the simulation
SS04	Long period 3D finite difference modeling of the Kobe mainshock (R. W. Graves)	Long-period 3-D FDM Short-period semi-empirical source: Wald (1996) basin: Miyakoshi (1997)	OS5, FKS, OSA, MRG, YAE, OS6 (vel.)	long-period, long-duration 3-D basin arrivals
SS05	3D waveform simulation in Kobe of the 1995 Hyogoken-nanbu earthquake by FDM using with discontinuous grids (S. Aoi)	Long-period: 3-D FDM with variable grid source: Sekiguchi et al (1998) basin: Iwata et al. (1998)	KBU, KB1-KB4, RKI (acc. & vel.)	3-D basin effects in the seismograms
SS06	Simulations of long-period ground motions during the 1995 Hyogoken-nanbu (Kobe) earthquake using 3D finite element method (Y. Hisada)	Long-period: 3-D FEM by Bao et al. (1998) source: original 3 point sources basin: Sano (1998)	KBU, KB1-KB4, RKI (acc. & vel.) [KBU is used for source calibration]	3-D basin effects in velocity seismograms
SS07	The 1995 Hyogo-ken Nanbu, Japan, earthquake simulated by the 3D finite difference method (J. Kristek)	Long-period: 3-D FDM with variable grid source: Sekiguchi et al (1998) basin: Iwata et al. (1998)	KBU, KB1-KB4, RKI (acc. & vel.)	3-D simulation of velocity seismograms
SS08	Ground motion simulation in the Kobe area during the 1995 Hyogo-ken Nanbu earthquake (T. Iwata)	Long-period: 3-D FDM by Pitarka et al. (1998) source: Sekiguchi et al (1998) basin: Iwata et al. (1998)	KBU, KB1-KB4, RKI (acc. & vel.)	3-D basin effects and source effects on ground motions in near-source area
SS09	3-D wave propagation analysis in Kobe referring to "The basin-edge effect" (S. Matsushima)	Long-period: 3-D FDM by Graves (1996) source: original 4 asperities basin: reflection surveys (Kawase & Matsushima 1998)	KBU, KB1-KB4, RKI (acc. & vel.)	3-D basin-edge effect and source effect in velocity seismograms
SS13	Stochastic simulations based on statistics of strong ground motions (A.G. Tumarkin)	Whole-period stochastic method with multi asperities Source: original from Kamae & Irikura (1998) and others Ground: 1-D theory + observed	KBU, KB1-KB4, RKI OS5, FKS, OSA, MRG, YAE, OS6 (acc. & vel.)	to test applicability of the modified stochastic approach

Table 2 List of submitted papers of S.S. for Kobe from SS14 to SS22 and their simulation outline

SS ##	Title of the paper (first author)	Method and Model	Simulated sites (values)	Main focus of the simulation
SS14	Computation of the strong motions during the 1995 Hyogo-ken Nanbu earthquake, combining the k-square spectral source model and the discrete wavenumber technique (C. Berge-Thierry)	Whole-period: k ² source model with DWM Green's function Source: Sekiguchi et al (1998) Ground: Iwata et al (1996) & shallow part from N-value (Ohta & Goto, 1970)	KBU, KB1-KB4, RKI (acc.)	Broadband accelerogram simulation; accelerogram with omega-square spectral shape; nonlinearity of shallow sediments accounted for horizontal strong motion in Kobe
SS15	Simulation of strong ground motion using empirical Green's function method (K. Kamae)	Whole-period: Empirical Green's function method Source: original 3 asperities Ground: in aftershock records	KBU (acc.)	(Not available from the authors)
SS16	The empirical Green's function method by using simulated waveforms (Z.X. Zhao)	Whole-period: stochastic Green's function method with Herrman's (1979) source time Source: original 3 asperities Ground: original 2-D	KBU, KB1-KB4, RKI (acc. & vel.)	(Not available from the authors)
SS17	Simultaneous simulation test against observed ground motions of the 1995 Hyogo-ken Nanbu earthquake on the basis of wave propagation in multi-layered half space (M. Kawano)	Whole-period: theoretical Green's function of random media + 1-D surface response Source: modified from Sekiguchi et al (1998) Ground: Iwata et al. (1996) & others, nonlinearity considered	KBU, KB2, RKI (acc.)	(Not available from the authors)
SS18	Kobe simulation by hybrid methods (I. Oprsal)	Whole-period: hybrid method of stochastic Green's function and 2-D FDM Source: Kamae & Irikura (1998) Ground: Pitarka et al. (1997) & Horike et al. (1996)	KBU, KB1-KB4, RKI (vel.) [KBU & MRG are used as reference]	Combination of the 3 asperity source, 1-D crustal path, and 2-D basin-edge effects
SS19	Simulation of strong ground motions during the 1995 Hyogo-ken Nanbu earthquake using 2-D seismic profiles at six sections in Kobe City (K. Koyamada)	Whole-period: 2-D FEM + 1-D effective-stress method for surface response Source: (deconvolved) Ground: original based on reflection surveys	KB1-KB4, RKI (acc. & vel.) [KBU is used as reference]	2-D basin effects on the strong motion; Comparison of PGA and PGV distribution with damage ratios of structures
SS20	Simulation of ground motion at Kobe case using the non-linear dynamic response (T. Kuriyama)	Whole-period: 2-D FEM + 1-D equivalent linear method for surface response Source: (deconvolved) Ground: original	KB1-KB4, RKI, OS5, OSA, MRG, YAE, OS6 (acc. & vel.) [KBU & FKS are used as reference]	2-D basin effects and 1-D nonlinear response of shallow soil layer in the acceleration seismograms
SS21	Earthquake response evaluation of sites in liquefied area (S. Miwa)	Whole-period: 1-D effective stress and equivalent linear method Source: (deconvolved) Ground: CAGDK (1998)	KB1-KB4, RKI (acc. & vel.) [both hole PIS is used as reference]	(Not available from the authors)
SS22	Simulations of Kobe case and Osaka case by the empirical Green's function method considering nonlinear behavior of surface ground (I. Suetomi)	Whole-period: Kobe=1-D equivalent linear; Osaka=empirical Green's function method + 1-D equivalent linear Source: Kobe=deconvolved; Osaka=Kamae & Irikura (1998) Ground: boring data and Miyakoshi (1997)	KB1-KB4, RKI, RKI, OS5, OSA, MRG, YAE, OS6 (vel.) [KBU is used as reference]	(Not available from the authors)

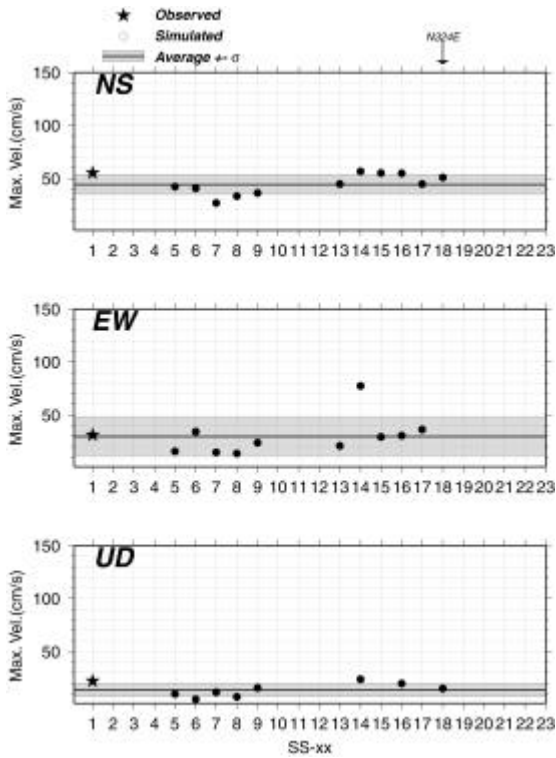


Fig.1 PGVs of all the submitted synthetics at KBU.

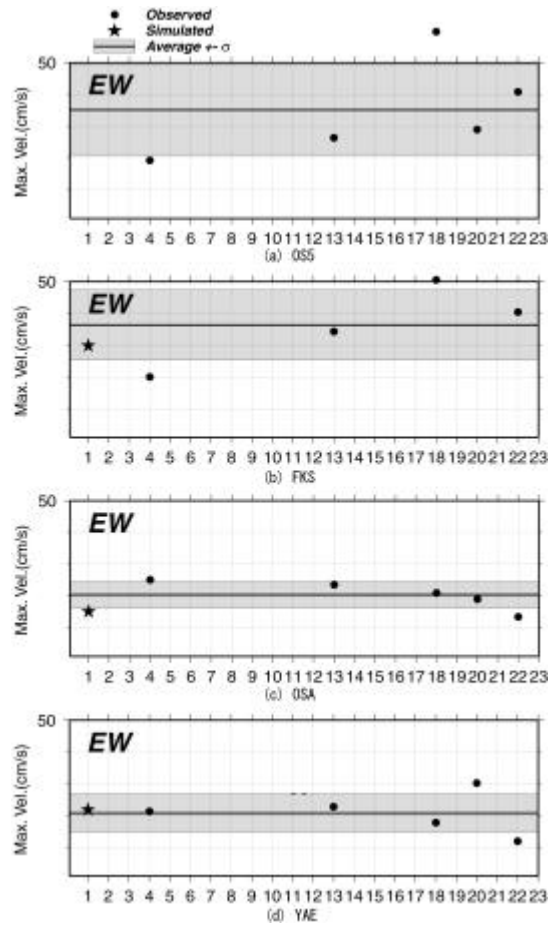


Fig.3 PGVs of all the submitted synthetics at four sites in the Osaka line, EW component.

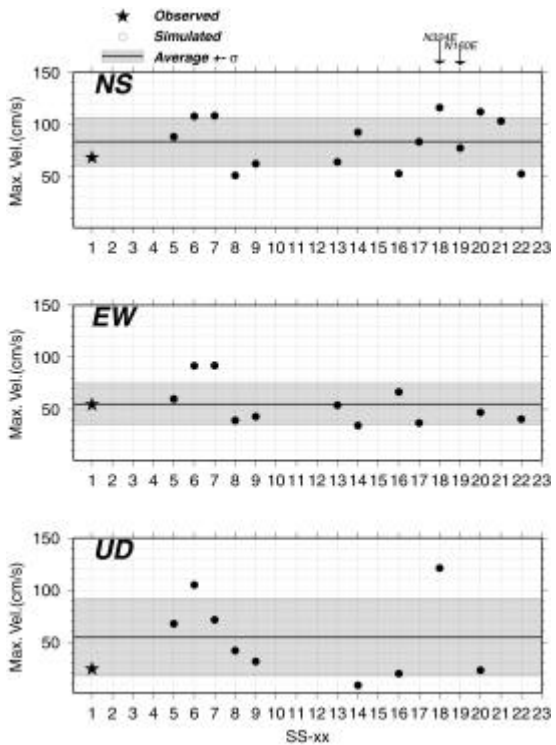


Fig.2 PGVs of all the submitted synthetics at RKI.

Table 3 Observed and averaged PGVs, standard deviations, and coefficient of variation (NS/EW/UD).

Site	Obs. (cm)	Ave. (cm/s)	S.D. (cm/s)	C.O.V. (%)
KBU	55/31/22	44/30/14	9/18/ 6	20/60/43
KB1	-	72/52/55	28/12/31	40/23/56
KB2	-	87/59/60	30/24/36	34/41/60
KB3	-	102/60/57	30/25/30	29/42/53
KB4	-	82/61/60	29/18/43	35/30/72
RKI	55/68/24	84/55/55	23/20/55	27/36/100
OS5	-	32/35/20	7/14/13	22/40/65
FKS	31/30/10	32/36/17	5/11/ 1	16/30/ 6

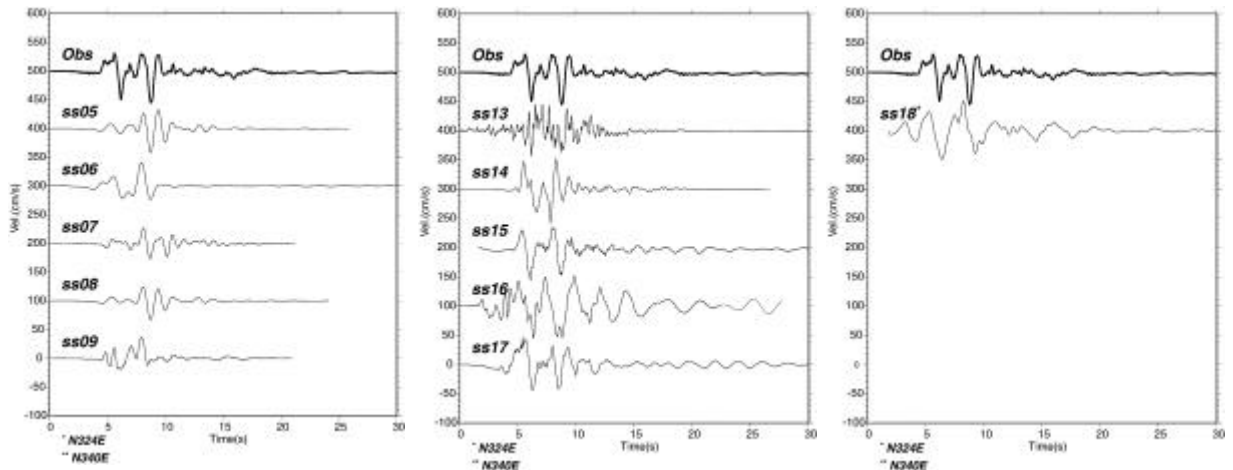


Fig.4 Velocity waveforms observed (thick line) and simulated (thin line) at KBU, NS component.

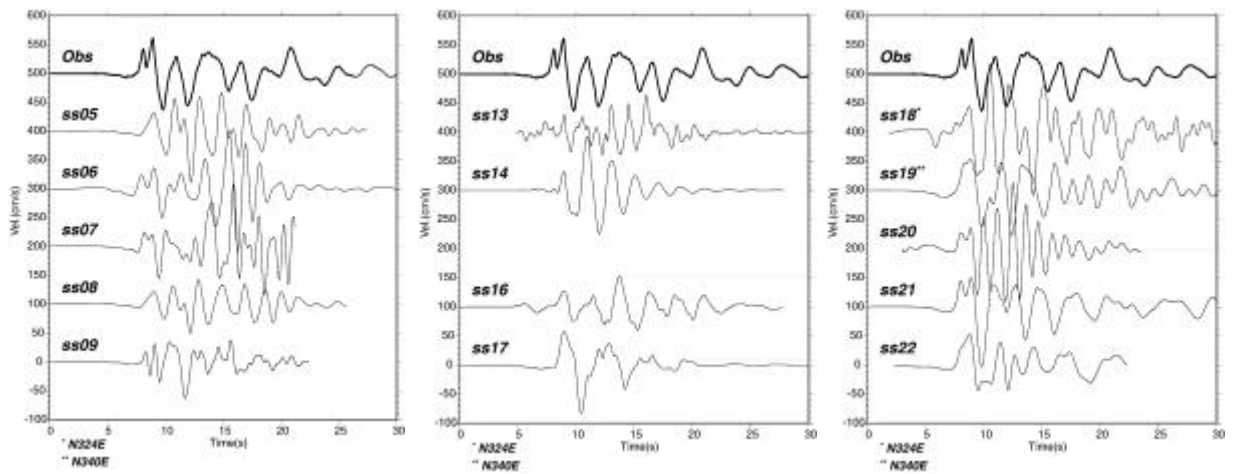


Fig.5 Velocity waveforms observed (thick line) and simulated (thin line) at RKI, NS component.

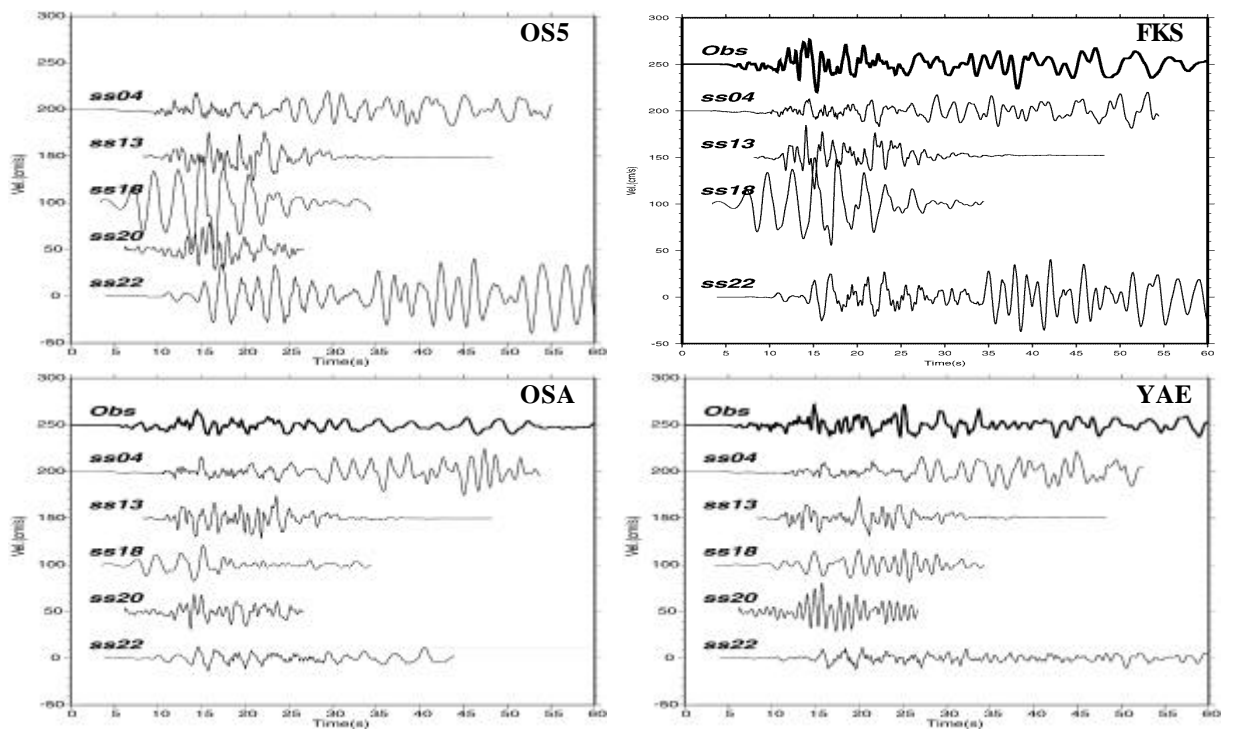


Fig.6 Velocity waveforms observed (thick line) and simulated (thin line) along the Osaka line, at OS5, FKS, OSA, and YAE, EW component.